

Impact of solar tower design parameters on sCO₂-based solar tower plants

Buck, Reiner; Giuliano, Stefano

In: 2nd European sCO₂ Conference 2018

This text is provided by DuEPublico, the central repository of the University Duisburg-Essen.

This version of the e-publication may differ from a potential published print or online version.

DOI: <https://doi.org/10.17185/duepublico/46098>

URN: <urn:nbn:de:hbz:464-20180827-151852-6>

Link: <https://duepublico.uni-duisburg-essen.de:443/servlets/DocumentServlet?id=46098>

License:



This work may be used under a [Creative Commons Namensnennung 4.0 International](https://creativecommons.org/licenses/by/4.0/) license.

IMPACT OF SOLAR TOWER DESIGN PARAMETERS ON sCO₂-BASED SOLAR TOWER PLANTS

Reiner Buck*
DLR, SF-ST5
Stuttgart, Germany
reiner.buck@dlr.de

Stefano Giuliano
DLR
Stuttgart, Germany

ABSTRACT

Integrating high efficiency sCO₂ power cycles into solar tower plants is characterized by high upper temperature and low temperature spread of the cycle working fluid sCO₂. New heat transfer media (HTM) are required, enabling higher temperatures and low cost storage. The present study evaluates modular solar tower plants using solid particles as HTM, allowing temperatures up to 1000°C. In a parameter study the influence of HTM temperatures on levelized cost of electricity (LCoE) is evaluated.

The results show a significant impact of the HTM temperature selection, mainly governed by the HTM temperature difference. A high temperature difference results in reduced LCoE. The most important factors for this reduction are the reductions in particle inventory, storage containment, and particle-sCO₂ heat exchanger. This reduction is partially offset by an increase in heliostat field and tower cost.

The results indicate that the use of solid particles for solar high efficiency sCO₂ power cycles offers unique advantages due to the wide temperature range of the particles.

INTRODUCTION

Power cycles using supercritical (sCO₂) as working fluid promise to become a competitive solution for future power cycles. The turbomachinery of such cycles is significantly smaller than that of comparable steam power cycles, and there is a potential for higher thermal efficiencies at elevated temperatures. In addition, the smaller components might improve the operational flexibility as there is less thermal inertia in the turbomachinery. Furthermore, the smaller components promise to reduce the specific power cycle cost.

For the application with concentrating solar power (CSP) systems the high efficiency potential makes the sCO₂ cycles especially attractive, as the “expensive” solar energy input can be reduced accordingly. This would result in smaller heliostat fields, receivers and storage systems, thus reducing investment cost. The intended high efficiency sCO₂ cycles are characterized by two aspects:

- high upper temperature of the cycle working fluid sCO₂, typically above 600°C

- low temperature spread of the cycle working fluid sCO₂, typically in the range of 150K

State-of-the-art heat transfer media (HTM) like “solar salt”, a mixture of 60% NaNO₃ and 40% KNO₃, are not suitable for such high temperatures. Therefore, new HTM are required. These new HTM should also provide cost-effective storage capabilities.

In the US study on the next generation of CSP plants (“Concentrating Solar Power Gen3 Demonstration Roadmap”) [1] sCO₂ cycles are foreseen for solar power generation, operating at upper temperatures as high as 715°C. Three potential candidates for the HTM are identified: new molten salt mixtures, solid particles and pressurized gases. For the last option, solid particles are also favored as storage material.

All three candidate HTM offer flexibility in the selection of the lower and upper temperature levels, which influence the layout and operating conditions of the solar power plant. The selection of these temperatures influences mainly the following aspects: area of the primary heat exchanger of the sCO₂ cycle, receiver efficiency, HTM mass flow, storage mass and volume, thermal insulation. Some of these parameters have a significant impact on investment cost.

In the present analysis, solid particles are selected as HTM. The reason for this selection is the extremely wide acceptable temperature range, up to 1000°C and without a limitation at lower temperatures (e. g. no freezing issues). The low cost of the particles enables also direct use as storage material.

The objective of this paper is the evaluation of trends when a high efficiency sCO₂ cycle is combined with a CSP system using a new HTM. The analysis is based on several simplified assumptions, as many of the components are not developed yet and therefore detailed cost and performance are not available. The results should be understood as trend indicators, not as absolute numbers.

MODEL AND ASSUMPTIONS

For the analysis, a solar tower system with a power rating of 100 MW_e is considered. The plant consists of 14 solar tower modules (multi-tower design) delivering heat to a single central power station. Each solar tower module consists of a heliostat

field, a tower with a receiver on top, a hot and cold storage containment and the heat transfer medium loop. The components of the plant are described in the following sections.

Power Cycle

The power cycle is a sCO₂ cycle in recompression configuration, with reheat and intercooling. The cycle layout was developed by SIEMENS and is shown in Figure 1. Further characteristics of the cycle are discussed in [2] in more detail. The primary heat exchanger, where the solar heat is introduced, consists of the main heat exchanger (item 6 in Figure 1) and the reheater (item 11 in Figure 1). In the main heat exchanger, sCO₂ is heated from 454°C to 605°C, in the reheater sCO₂ is heated from 502°C to 605°C. The sophisticated cycle configuration results in an excellent cycle efficiency of 50%, without increasing the cycle temperatures too much. With this efficiency, a thermal input power of 200MW_{th} is required from the solar subsystem. For the layout and costing of the primary

heat exchanger it is considered as a single heat exchanger. Then the average inlet temperature of the main and reheat section of 478°C is used.

Currently, no reliable cost data for such a large power cycle is available. In [3] the specific cost of several sCO₂ cycles is estimated. High efficiency configurations of the investigated sCO₂ cycles were estimated in the range from 1097\$/kW_e to 1392\$/kW_e. For the shown complex sCO₂ power cycle configuration, only preliminary cost estimates can be made. For the present analysis, the primary (particle-to-sCO₂) heat exchanger is treated as a separate cost item, as the cost of this heat exchanger is strongly influenced by the selected temperature range. For the cost of the remainder of the sCO₂ cycle, a fixed specific cost of C_{sp,cycle} = 1000€/kW_e is assumed. This results in a power cycle cost C_{pc} of 100 Mio € (excluding primary heat exchanger).

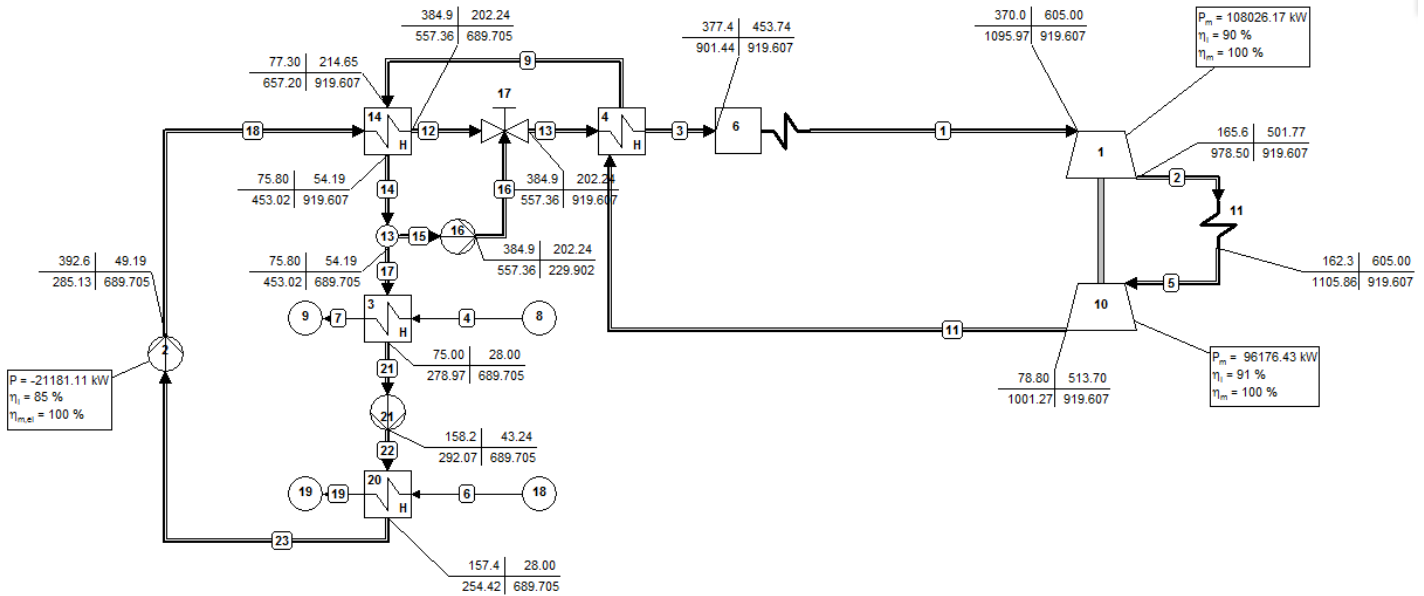


Figure 1: Configuration of the high efficiency / high temperature sCO₂ cycle

Solar Tower Module Description

Each of the 14 solar tower modules consists of a receiver with a design point (DP) power of 50MW_{th} and the corresponding heliostat field and thermal storage. A scheme of a module is shown in Figure 2.

The module power of 50MW_{th} at DP conditions results in a total thermal system power of 700MW_{th}. With the power cycle demand of 200MW_{th} this represents a solar multiple of 3.5.

For the analysis, a site in Northern Chile with an annual direct normal insolation (DNI) of 3583kWh/m²a is assumed. This is an extremely good solar site, however the trend results should be representative for other sites as well.

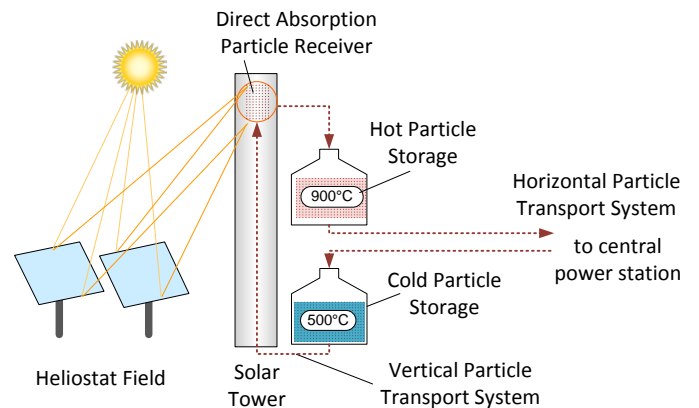


Figure 2: Solar tower module scheme

Heat Transfer and Storage Medium

Bauxite particles are assumed as heat transfer and storage medium, since these particles are relatively inexpensive and allow flexible selection of temperature ranges up to 1000°C. Above this temperature, sintering effects might create problems in particle handling. Also, a lower temperature limit does not exist, and therefore electrical heat tracing is not necessary to avoid HTM freezing. Simplified assumptions for the particle properties are:

$$\text{heat capacity: } c_{p,part} = 1200 \text{ J/kgK}$$

$$\text{particle bulk density: } \rho_{part} = 2000 \frac{\text{kg}}{\text{m}^3}$$

Such bauxite particles are produced in huge quantities, e. g. for use in fracking or casting processes. A specific particle cost of $C_{sp,part} = 1\text{€}/\text{kg}$ is assumed.



Figure 3: Solid bauxite particles used as HTM

Thermal Storage System

For the solar tower system, a thermal storage time of 12h full load operation was assumed, resulting in a total thermal storage capacity E_{st} of 2.4 GWh. This storage capacity is evenly distributed over all solar tower modules. The hot and cold storage containments are either installed inside the tower (eventually using the tower walls as containment walls, with inner insulation) or close to the tower.

Thermal losses through the thermal insulation are neglected. Such losses are usually relatively small. This simplification is also justified since the cost of the insulation is assumed temperature-dependent, i. e. for higher temperatures an improved quality insulation is foreseen.

The particle inventory per module is calculated as

$$m_{st} = \frac{E_{st}}{n_{mod} \cdot c_{p,part} \cdot (T_{r,ex} - T_{r,in})}$$

Another 10% of this particle mass is added to account for particles in other components, e. g. the transport containments.

The cost of the particle inventory C_{part} is then calculated as

$$C_{part} = 1.1 \cdot m_{st} \cdot C_{sp,part}$$

The cost of the storage containment C_{stc} is calculated from the surface area A_{stc} of the containment. A cylindrical containment with the cylinder height being twice the cylinder diameter is assumed. From the particle inventory, the volume of a fully charged containment is calculated, and then the cylinder diameter and the surface area are derived. Then a temperature-dependent area-specific insulated structure cost $C_{sp,is}$ is calculated as follows:

$$C_{A,sp,is}(T_{st}) = 1000 + f_{ins} \cdot \frac{(T_{st} - 600)}{400}$$

The insulation factor f_{ins} describes the cost share of the thermal insulation. In the above formulation, the insulation cost is doubled when the storage temperature T_{st} (in K) is increased from 600°C to 1000°C. A value of $f_{ins} = 0.3$ is assumed for the insulation cost share. The storage containment cost is the sum of the cost of the hot and cold storage containments:

$$C_{stc} = A_{stc} \cdot C_{A,sp,is}(T_{r,ex}) + A_{stc} \cdot C_{A,sp,is}(T_{r,in})$$

The total cost of the storage system C_{st} is then calculated as

$$C_{st} = C_{part} + C_{stc}$$

Solar Receiver

The receiver technology is based on the centrifugal particle receiver technology CentRec[®] [4]. This receiver technology is currently under development at DLR. The receiver is based on the direct absorption principle, meaning that the dark bauxite particles are irradiated directly by the concentrated solar power and get heated from the absorbed radiation.

A first demonstration receiver with about 2.5MW_{th} peak power is installed at the DLR solar tower test facility in Jülich, Germany. Due to constraints of the test platform in the solar tower test facility, which is located about midway up the tower, a thermal power output of up to 500kW_{th} is expected. More than 30h of solar testing has been carried out so far, and receiver outlet temperatures up to 775°C have been achieved [4]. Solar tests will continue in spring 2018 with the goal to demonstrate the design outlet temperature of 900°C.

The receiver is characterized by a circular aperture that is facing south, since the plant site is located in Chile on the southern hemisphere. The aperture area A_{ap} varies according to the selected temperature range and is determined during the solar system optimization. A simplified receiver model is considered, with the absorbed power $P_{r,abs}$ defined as a function of intercepted power $P_{r,int}$ and receiver exit temperature $T_{r,ex}$ by

$$P_{r,abs} = \alpha \cdot P_{r,int} - \varepsilon \sigma A_{ap} T_{r,ex}^4 - h A_{ap} (T_{r,ex} - T_{amb})$$

with

$$\text{effective solar absorptivity: } \alpha = 0.95$$

$$\text{effective thermal emissivity: } \varepsilon = 0.9$$

$$\text{convective heat loss coefficient: } h = 30 \text{ W/m}^2\text{K}$$

Note that in the above correlation all temperatures must be used in [K]. For the ambient temperature, a value of 300K is

taken. The receiver cost is described by two contributing factors: one depending only on the receiver aperture, another one depending on the surface area of the internal insulated structure and the receiver exit temperature. The surface area of the internal insulated structure is calculated for a cylindrical receiver chamber with a diameter of 1.3 times the aperture diameter and a depth of 2 times the aperture diameter. The area of the insulated structure $A_{r, is}$ is then composed of area of the cylinder wall and the area of the flat back wall of the cylinder. The total cost of the receiver system C_r is calculated as

$$C_r = 70000 \cdot A_{ap} + A_{r, is} \cdot C_{A, sp, is}(T_{r, ex})$$

Heliostat Field

The heliostat field consists of a large number of rectangular heliostats, tracked in two axes. The heliostat dimension is 12.84 m width and 9.45 m height. A reflectivity of 88% is assumed, accounting for the mirror reflectivity and an average dirt coverage of the mirrors. A specific cost $C_{sp, f}$ of 100 €/m² installed heliostat field is assumed.

For each temperature range, the heliostat field layout and the number of heliostats are optimized using the simulation tool HFLCAL [6]. A radially staggered field layout is selected. As a result, the total heliostat field area A_f is obtained.

The total cost of the heliostat field C_{field} is calculated as

$$C_f = A_f \cdot C_{sp, f}$$

Tower

A tower is required to locate the solar receiver at a suitable height above the heliostat field. The tower height is dominated by the heliostat field and receiver configuration, and is optimized together with other parameters.

The cost of the tower is assumed as

$$C_t = 128 \cdot H_t^{1.9174}$$

Heat Exchanger

A moving bed particle heat exchanger (Figure 4) is foreseen for the heating of the working fluid sCO₂ of the power cycle. In this heat exchanger type, the solid particles are moving slowly across the heat exchanger tubes, driven by gravity [6]. The mass flow is controlled by variable gate valves at the cold exit of the heat exchanger.

The required heat transfer area of this heat exchanger is calculated as

$$A_{HX} = \frac{P_{el} / \eta_{cycle}}{h_{HX} \cdot \Delta T_{log}}$$

In [6] convective heat transfer coefficients up to 240 W/m²K were measured for a tube bundle type heat exchanger with particle inlet temperatures ranging from 355°C to 470°C. Since the particle heat exchanger for a sCO₂ power cycle is operated at significantly higher temperatures, radiative heat transfer will be improving the heat transfer. Here, a

constant heat transfer coefficient h_{HX} of 300 W/m²K is assumed. The logarithmic temperature difference ΔT_{log} for a heat exchanger in cross-flow configuration is calculated based on the solid particle temperature selection and the power cycle temperature levels. The primary heat exchanger temperatures of the power cycle are 605°C for the sCO₂ outlet and 478°C for the sCO₂ inlet.

The primary heat exchanger material temperatures are mainly defined by the sCO₂ cycle conditions, as the highest heat transfer resistance will be between particles and tube material, i. e. the tube material temperatures will be quite independent of particle temperatures. Thus, the heat exchanger cost is only a function of the heat transfer area.

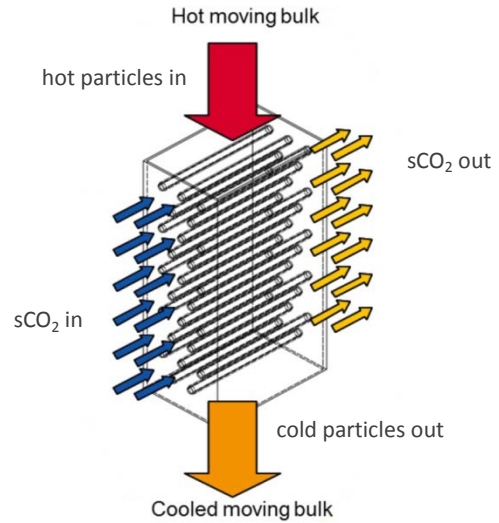


Figure 4: Moving bed particle heat exchanger

For the cost of the heat exchanger a correlation was derived using the MATCHE data base [8] assuming Inconel625 as tube material. With a correction factor the high pressure of the sCO₂ system, a translation from 2014 cost into actual cost and after converting from \$ to € this resulted in the following correlation:

$$C_{HX} = 128122 \cdot A_{HX}^{0.66}$$

Particle Transport System

The multitower system needs particle transportation in two ways: lifting the “cold” particles up to the receiver inlet (“vertical” particle transport) and transporting the particles between a solar tower module and the central power station (“horizontal” particle transport). After being cooled down in the central particle-sCO₂ heat exchanger, the cold particles are transported back to the solar tower modules and are either lifted up to the receiver (when enough solar power is available to heat the particles) or lifted to the inlet of the cold storage container. When more solar power is available than the power cycle takes, particles from the cold storage are lifted up to the receiver and, after being heated up, put into the hot storage. Particle transport downwards is always accomplished by gravitational flow.

Vertical particle transport

For the vertical particle transport a mine hoist system is foreseen. Repole et al. [9] have made a conceptual design for a mine hoist system for a solar demonstration system with a thermal capacity of 60MW_{th} . Since the selected solar tower module size is close to this capacity, this mine hoist design was taken as base value for the calculation of the cost for the specific configuration. Scaling factors are applied for conditions differing from the original design values. The used correlation is

$$C_{tr} = C_{tr,0} \cdot \left\{ 1 + k_T \left(\frac{T_l - T_{l,0}}{T_{l,0}} \right) \right\} \cdot \left\{ 1 + k_m \left(\frac{\dot{m} - \dot{m}_0}{\dot{m}_0} \right) \right\} \cdot \left\{ 1 + k_H \left(\frac{H_l - H_{l,0}}{H_{l,0}} \right) \right\}$$

with

$$C_{tr,0} = 425000\text{€ (converted from 523000\$)}$$

The original design values in [9] are:

$$T_{l,0} = 300^\circ\text{C (assumed, not clearly stated in [9])}$$

$$\dot{m}_0 = 128 \text{ kg/s}$$

$$H_{l,0} = 70\text{m}$$

The selected scaling factors are:

$$k_T = 0.1$$

$$k_m = 0.5$$

$$k_H = 0.2$$

Horizontal particle transport

For the transportation between the solar tower modules and the central power station a number of trucks are foreseen, each transporting insulated containers (one for hot and another for cold particles). One truck is serving one module. This is sufficient for the highest particle mass flows (i. e. the smallest temperature particle difference of 200K), for lower mass flows this is even oversized and might be reduced in further system optimization. The trucks are continuously operated whenever the power cycle is producing electricity, e. g. also during night time. As the paths between the solar tower modules and the central power block are clearly defined, fully autonomous trucks are foreseen. The cost of each truck system is estimated as $C_{tr,h} = 280000\text{€}$ and includes the truck and 6 insulated containers (3 for cold particles and 3 for hot particles). This enables continuous operation of the horizontal particle transport system, with one container discharged, one container being transported, and one container being charged at the same time.

Other Performance Assumptions

For simplicity reasons, thermal losses through the insulation are neglected, as they are usually very small: Also, the parasitic power consumption of the various components (rotation drive of cylindrical receiver, vertical and horizontal particle transport system, power cycle parasitics) was excluded from the analysis. While thermal losses might slightly increase

with higher temperatures, parasitic power will decrease as the particle mass flow will go down.

OPTIMIZATION OF SYSTEM CONFIGURATION

A number of system configurations are evaluated, with the levelized cost of electricity (*LCoE*) as the evaluation criteria.

The capital expenditures for a single tower module ($CAPEX_{mod}$) are calculated by

$$CAPEX_{mod} = C_f + C_t + C_r + C_{tr,v} + C_{tr,h} + C_{st}$$

For the calculation of the total capital expenditures (*CAPEX*) the cost of all modules is combined with the cost of the central power block (consisting of heat exchanger and power cycle), and contingencies of 30% are added to this sum:

$$CAPEX = 1.3 \cdot (n_{mod} \cdot CAPEX_{mod} + C_{HX} + C_{pc})$$

Annual operational expenditures (*OPEX*) are assumed as 2% of the total *CAPEX*. The annual electric power production is then calculated from the annual thermal energy as obtained from the HFLCAL layout optimization:

$$E_{el,annual} = E_{th,annual} \cdot \eta_{cycle}$$

The evaluation of the *LCoE* is based on a simplified annuity approach as follows:

$$LCoE = \frac{CAPEX \cdot f_{annuity} + OPEX}{E_{el,annual}}$$

The annuity factor $f_{annuity}$ is based on the interest rate and the depreciation period [9]. With an interest rate of 5% and a depreciation period of 25a an annuity factor of 7.1% is obtained.

Each configuration is defined by a specific receiver inlet and outlet temperature. For each temperature set, the solar subsystem is optimized for minimal *LcoE*. The following parameters are varied during the optimization: receiver aperture area, receiver tilt angle, tower height and field layout. A radially staggered field layout is assumed. The simulation tool HFLCAL [6] was used to determine the optimal parameters for each temperature set.

RESULTS

The parameter study was carried out using receiver inlet temperatures of 500°C , 600°C and 700°C . Temperature differences between receiver exit and inlet temperature were between 200°C and 500°C , with an upper limit for the receiver exit temperature of 1000°C .

Figure 5 shows the resulting *LCoE* for the selected parameter sets. It is obvious that the higher the receiver exit temperature the lower the *LCoE* is. For a given receiver exit temperature, lower receiver inlet temperatures result in lower *LCoE*. The *LCoE* difference between the best ($500^\circ\text{C}/1000^\circ\text{C}$) and the worst case ($500^\circ\text{C}/700^\circ\text{C}$) is about 9%.

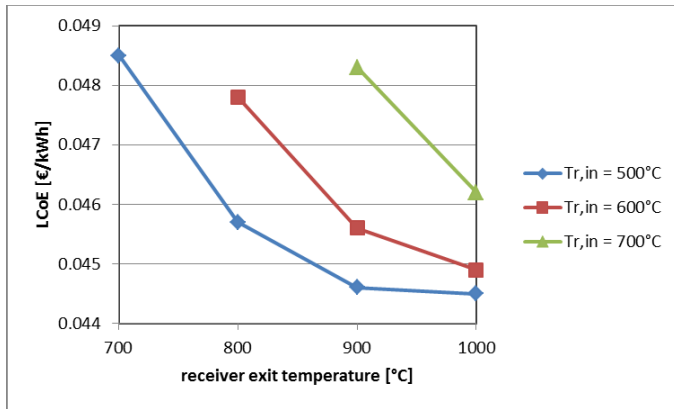


Figure 5: Levelized cost of electricity vs. temperature range

Showing the data in a different representation based on the temperature difference between receiver exit and inlet temperature (Figure 6) it is evident that this temperature difference is the dominant factor for the change in LCoE.

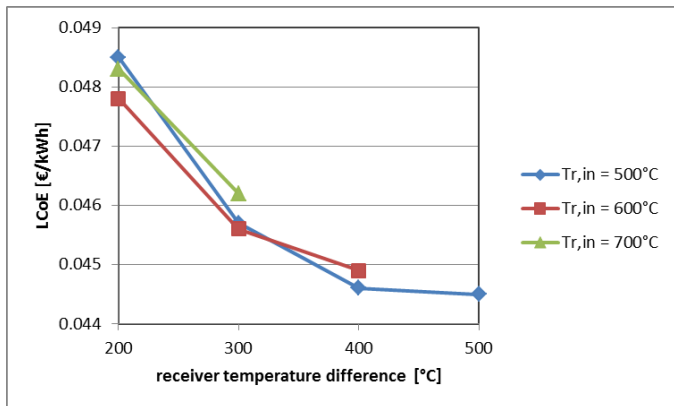


Figure 6: Levelized cost of electricity vs. temp. difference

Table 1: Detailed results of parameter study

receiver inlet temperature	[°C]	500	500	500	500	600	600	600	700	700
receiver exit temperature	[°C]	700	800	900	1000	800	900	1000	900	1000
component cost										
heliostat field	[Mio €]	115.2	116.9	120.3	123.3	118.6	121.6	124.2	120.9	124.0
tower	[Mio €]	19.9	21.6	21.8	23.0	19.8	20.7	22.1	20.5	22.5
receiver	[Mio €]	32.9	31.4	31.5	30.6	32.5	31.4	31.1	32.3	30.7
vertical particle transport	[Mio €]	9.7	7.8	6.8	6.3	10.0	8.0	7.1	10.4	8.4
horizontal particle transport	[Mio €]	3.9	3.9	3.9	3.9	3.9	3.9	3.9	3.9	3.9
particle-sCO ₂ heat exchanger	[Mio €]	39.4	31.4	27.2	24.4	26.5	23.2	21.0	20.8	18.9
sCO ₂ power cycle (excl. HX)	[Mio €]	100.0	100.0	100.0	100.0	100.0	100.0	100.0	100.0	100.0
particle inventory	[Mio €]	43.1	28.7	21.5	17.2	43.1	28.7	21.5	43.1	28.7
storage containments	[Mio €]	20.3	16.1	13.8	12.3	21.9	17.3	14.7	23.4	18.4
LCOE	[€/kWh]	0.0485	0.0457	0.0446	0.0445	0.0478	0.0456	0.0449	0.0483	0.0462

Figure 7 shows the cost contributions of the most important factors for the LCoE change. The shown characteristic is mainly resulting from a significant cost decrease in the storage cost and in the heat exchanger cost, when the temperature difference is increased. A minor cost decrease occurs in the particle transport system, mainly due to reduced mass flow requirements.

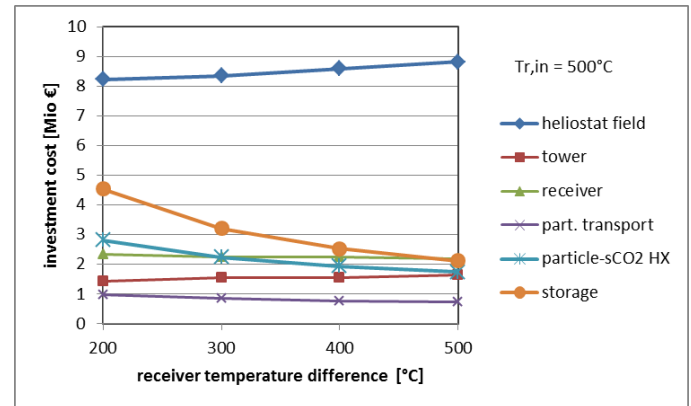


Figure 7: Component cost vs. temperature difference

On the other hand, the cost of heliostat field and tower increase with increasing receiver exit temperature. This is caused by decreasing receiver efficiency, requiring more heliostats and a higher tower to deliver the required thermal power. When the receiver exit temperature is increased, higher area-specific thermal losses occur in the receiver. In the solar system optimization this leads to smaller receivers, which is why the receiver cost decrease. More details on the component cost are given in Table 1.

CONCLUSIONS

Integrating high efficiency sCO₂ power cycles into solar tower plants is characterized by high upper temperature of the cycle working fluid sCO₂ (typically above 600°C) and low temperature spread of the cycle working fluid sCO₂, typically in the range of 150K. This requires the use of new HTM, suitable for higher temperatures and featuring low cost storage. The present study evaluates modular solar tower plants using solid particles as HTM, allowing HTM temperatures up to 1000°C. In a parameter study the influence of the lower and upper HTM temperature on LCoE was evaluated.

The results show a significant impact of the HTM temperature selection, mainly governed by the HTM temperature difference. A high temperature difference results in reduced LCoE. The most important factors for this reduction are the reductions in particle inventory, storage containment, and particle-sCO₂ heat exchanger. This reduction is partially offset by an increase in heliostat field and tower cost.

The results indicate that the use of solid particles for solar high efficiency sCO₂ power cycles offers unique advantages due to the wide temperature range of the particles. In addition, the modular solar tower design will allow simple adaptation to other power levels and capacity factors.

It should be stated that several of the used cost correlations are “best guesses”, as currently no sound database exists for many of the new components. These correlations should be refined by future work to improve the quality of the results.

NOMENCLATURE

Symbols:

Symbol	unit	description
<i>A</i>	[m ²]	area
<i>C</i>	[€]	cost
<i>c_p</i>	[J/kgK]	heat capacity
<i>E</i>	[J]	energy
<i>H</i>	[m]	tower height
<i>n_{mod}</i>	[-]	number of solar tower modules
<i>LCoE</i>	[€/MWh]	levelized cost of electricity
<i>P</i>	[W]	power
<i>T</i>	[°C]; [K]	temperature
<i>ρ</i>	[kg/m ³]	density
<i>η</i>	[-]	efficiency

Subscripts:

<i>abs</i>	absorbed
<i>amb</i>	ambient
<i>annual</i>	annual value
<i>ap</i>	aperture
<i>cycle</i>	sCO ₂ power cycle
<i>el</i>	electric
<i>ex</i>	exit
<i>f</i>	field
<i>h</i>	horizontal
<i>HX</i>	(primary) heat exchanger

<i>in</i>	inlet
<i>int</i>	intercepted
<i>is</i>	insulated structure
<i>mod</i>	(solar tower) module
<i>part</i>	particle
<i>pc</i>	power cycle
<i>r</i>	receiver
<i>st</i>	storage
<i>stc</i>	storage containment
<i>sp</i>	specific
<i>th</i>	thermal
<i>tr</i>	transport
<i>t</i>	tower
<i>v</i>	vertical

ABBREVIATIONS

CAPEX:	capital expenditures
CSP:	concentrating solar power
DNI:	direct normal insolation
DP:	design point
HTM:	heat transfer medium
OPEX:	operational expenditures

ACKNOWLEDGEMENTS

The author would like to thank Stefano Giuliano and Lars Amsbeck for valuable discussions on the performance and cost assumptions.

REFERENCES

- [1] Concentrating Solar Power Gen3 Demonstration Roadmap; Technical Report NREL/TP-5500-67464, January 2017. Available at www.nrel.gov/publications.
- [2] Glos, S., Wechsung, M., Wagner, R., Heidenhof, A., Schlehuber, D. (2018). Evaluation of sCO₂ Power Cycles for Direct and Waste Heat Applications, 2nd European supercritical CO₂ Conference, August 30-31, 2018, Essen, Germany (to be published)
- [3] Carlson, M. D., Middleton, B. M., Ho, C. K. (2017). Techno-economic Comparison of Solar-driven sCO₂ Brayton Cycles using Component Cost Models Baselined with Vendor Data and Estimates, PowerEnergy2017-3590, Proc. ASME PowerEnergy2017, June 26-30, 2017, Charlotte, NC, USA
- [4] Ebert, M., Amsbeck, L., Jensch, A., Hertel, J., Rheinländer, J., Trebing, D., Uhlig, R., Buck, R. (2016). Upscaling, Manufacturing and Test of a Centrifugal Particle Receiver. PowerEnergy2016-59252, Proc. ASME Energy Sustainability Conference, 26.-30. June 2016, Charlotte, United States.
- [5] Ebert, M., Amsbeck, L., Buck, R., Rheinländer, J., Schlögl-Knothe, B., Schmitz, S., Sibus, M., Stadler, S., Uhlig, R. (2018). First On-sun Tests of a Centrifugal Particle Receiver System, PowerEnergy2018-7166, Proc. ASME 2018 Power and Energy Conference (PowerEnergy2018), June 24-28, 2018, Lake Buena Vista, FL, USA (to be published)
- [6] Schwarzbözl, P., Pitz-Paal, R. and Schmitz, M. (2009) Visual HFLCAL - A Software Tool for Layout and

Optimisation of Heliostat Fields. Proceedings SolarPACES 2009, Berlin.

[7] Baumann, T., Zunft, S. (2014). Experimental Investigation on a Moving Bed Heat Exchanger used for discharge of a particle-based TES for CSP. Eurotherm Seminar #99 - Advances in Thermal Energy Storage. Eurotherm Seminar #99, 28.05.-30.05.2014, Lleida, Spain. ISBN 978 84 697 0467 7

[8] <http://matche.com/equipcost/Exchanger.html> (last visited 22.06.2018)

[9] Repole, K. D., Jeter, S. M. (2016). Design and Analysis of a High Temperature Particulate Hoist for Proposed Particle Heating Concentrator Solar Power Systems. ASME Energy Sustainability 2016. doi:10.1115/ES2016-59619.

[10] Roy, A., Meinecke, W., Blanco, M. (1997). "Introductory Guidelines for Preparing Reports on Solar Thermal Power Systems", SolarPACES Rep. No. III-3/97.